Published in final edited form as:
Arch Neurol. 2010 November ; 67(11): 1336–1344. doi:10.1001/archneurol.2010.149.

Regionally Selective Atrophy after Traumatic Axonal Injury

Matthew A Warner, BS[*], **Teddy Youn, MD**[#], **Tommy Davis, PhD, MPH**[*], **Alvin Chandra, BS**[*], **Carlos Marquez de la Plata, PhD**[ˈ], **Carol Moore, MA**[*], **Caryn Harper, MS**[*], **Christopher J Madden, MD**[+], **Jeffrey Spence, PhD**[ǀ], **Roderick McColl, PhD**[¨], **Michael Devous, PhD**[¨], **Richard King, MD, PhD**[}], and **Ramon Diaz-Arrastia, MD, PhD**[*]

[*]Departments of Neurology University of Texas Southwestern Medical Center, Dallas, TX, USA

[+]Neurological Surgery University of Texas Southwestern Medical Center, Dallas, TX, USA

[ǀ]Clinical Science University of Texas Southwestern Medical Center, Dallas, TX, USA

[¨]Radiology University of Texas Southwestern Medical Center, Dallas, TX, USA

[#]Department of Neurology, University of Washington, Seattle, WA, USA

[ˈ]University of Dallas, Center for Brain Health, Dallas, TX, USA

[}]Department of Neurology, University of Utah, Salt Lake City, UT, USA

Abstract

Objectives—To determine the spatial distribution of cortical and subcortical volume loss in patients with diffuse traumatic axonal injury and to assess the relationship between regional atrophy and functional outcome.

Design—Prospective imaging study. Longitudinal changes in global and regional brain volumes were assessed using high-resolution magnetic resonance imaging (MRI)-based morphometric analysis.

Setting—Inpatient traumatic brain injury unit

Patients or Other Participants—Twenty-five patients with diffuse traumatic axonal injury and 22 age- and sex-matched controls.

Main Outcome Measure—Changes in global and regional brain volumes between initial and follow-up MRI were used to assess the spatial distribution of post-traumatic volume loss. The Glasgow Outcome Scale – Extended was the primary measure of functional outcome.

Results—Patients underwent substantial global atrophy with mean brain parenchymal volume loss of 4.5% (95% Confidence Interval: 2.7 – 6.3%). Decreases in volume (at a false discovery rate of 0.05) were seen in several brain regions including the amygdala, hippocampus, thalamus, corpus callosum, putamen, precuneus, postcentral gyrus, paracentral lobule, and parietal and

Corresponding Author: Ramon Diaz-Arrastia, MD, PhD Department of Neurology, UTSW 5323 Harry Hines Blvd. Dallas, Texas 75390-9036 Ramon.Diaz-Arrastia@UTSouthwestern.edu Telephone: 214-648-6721, Fax: 214-648-6320.

Financial Disclosure: The authors report no financial conflicts of interests.

Author Contributions: All authors had full access to the data in the study and take full responsibility for data integrity, data analysis, and interpretation of results. *Study concept and design*: Warner, Youn, Moore, Harper, McColl, Devous, and Diaz-Arrastia. *Acquisition of Data*: Warner, Youn, Davis, Marquez de la Plata, Moore, Harper, Madden, McColl, and Devous. *Analysis and interpretation of data*: Warner, Youn, Davis, Chandra, Marquez de la Plata, Spence, King, and Diaz-Arrastia. *Drafting of manuscript*: Warner and Diaz-Arrastia. Critical revision of the manuscript for important intellectual content: Warner, Youn, Davis, Chandra, Marquez de la Plata, Moore, Harper, Madden, Spence, McColl, Devous, King, and Diaz-Arrastia. *Statistical analysis*: Warner and Spence. *Obtained funding:* Warner, Youn, and Diaz-Arrastia. *Administrative, technical, and material support*: Chandra, Marquez de la Plata, Moore, Harper, Madden, McColl, Devous, and King. *Study Supervision*: Warner, Youn, Davis, and Diaz-Arrastia.

frontal cortices, while other regions such as the caudate and inferior temporal cortex were relatively resistant to atrophy. Loss of whole brain parenchymal volume was predictive of long-term disability, as was atrophy of particular brain regions including the inferior parietal cortex, pars orbitalis, pericalcarine cortex, and supramarginal gyrus.

Conclusion—Traumatic axonal injury leads to substantial post-traumatic atrophy that is regionally selective rather than diffuse, and volume loss in certain regions may have prognostic value for functional recovery.

INTRODUCTION

Traumatic brain injury (TBI) is a major cause of death and disability worldwide, with 235,000 hospitalizations reported each year in the United States alone.[1] A common consequence of TBI is cerebral atrophy, which progresses over months and possibly years after injury.[2-10] The predominant view is that post-traumatic atrophy is a consequence of direct injury to the neuron body, or soma, which subsequently undergoes cytotoxic or apoptotic cell death.[11] However, it is now evident that significant loss of cerebral volume occurs even in those without focal lesions, suggesting that atrophy may result from diffuse traumatic axonal injury (TAI) with secondary Wallerian degeneration and delayed neuronal cell death, rather than direct damage to neuronal cell bodies.[9] As axons and soma differ substantially in cellular and molecular features such as expression of ion channels, cytoskeletal proteins, and bioenergetics, it is likely that future neuroprotective therapies will need to be separately tailored towards axonal or somatic injury.

Few studies have examined the spatial distribution of atrophy after TBI, and it remains unclear if volume loss is diffuse or regionally selective.[10,12-14] Moreover, no studies have assessed regional volume changes in patients with predominantly TAI. There are several challenges to quantifying the distribution of post-traumatic atrophy, including inter-subject anatomic variation and focal trauma that often coexists with diffuse lesions leading to regional shape distortion and complications with image registration and tissue segmentation.

Despite this, several quantitative MRI techniques have been applied to TBI. Region of interest analysis involves manually tracing readily identifiable structures based on *a priori* designation of tissue boundaries[3] and is limited in its ability to quantify less discrete neuroanatomic regions. To overcome this, methods have been developed that analyze brain tissue on a voxel-wise or whole brain approach such as voxel-based morphometry (VBM)[5,8,14,15] and tensor-based morphometry (TBM),[10,13] noting atrophy after TBI in several prominent white matter tracts and subcortical gray matter regions. However, voxel-wise approaches have several limitations, including low sensitivity for cortical atrophy and inadequacies in delineating gray matter from white. Moreover, few studies have longitudinally assessed atrophy after trauma,[6,10,14,16] and only two have examined regional variations in volume loss.[10,14] Existing longitudinal data rely on initial MRI scans that were performed several months after injury, and no study has assessed the progression of atrophy beginning acutely (within 1 week) after injury.

Recently, several automated approaches have been developed which allow for improved quantification of brain tissue. The *FreeSurfer* image analysis suite, available online (http://surfer.nmr.mgh.harvard.edu), allows for automated parcellation of cortical and subcortical gray and white matter. Unlike the aforementioned voxel-wise approaches, *FreeSurfer* allows for delineation of atlas-derived brain regions and improved quantification of cortical surfaces. It has been validated in epilepsy,[17] dementia,[18] Alzheimer's disease,[19] major depressive disorder,[20] and pediatric TBI[12] among others. To our knowledge, this is the first application of *FreeSurfer* morphometry to adult TBI.

The primary goal of this investigation was to quantify cerebral atrophy in patients with TAI using global and regional metrics, thereby determining if certain brain regions are selectively vulnerable to atrophy after trauma. We hypothesized that global measures of brain volume would show significant atrophy after injury, and that particular cortical and subcortical regions would undergo higher rates of volume loss. We also aimed to assess the relationship between atrophy and functional outcome, hypothesizing that volume loss in particular regions would be predictive of poor outcome.

METHODS

Subjects

This study was approved by the Institutional Review Board at the University of Texas Southwestern Medical Center in Dallas, Texas. From September 2005 to October 2008, 31 patients with TBI were recruited. Inclusion criteria included (1) injury mechanism consistent with TAI (involving high-speed acceleration-deceleration or rotational forces), (2) age 16 – 65, (3) hemodynamically stable for transfer to scanner, (4) Marshall grade II or post-resuscitation Glasgow Coma Scale (GCS) score < 13 with normal CT, and (5) able to provide informed written consent or obtain consent from a legally authorized representative. Exclusion criteria included (1) any focal, mixed, or high-density lesion > 10 ml, (2) midline shift > 3 mm at the level of septum pellucidum on admission CT, (3) penetrating head injury, (4) injury requiring craniectomy or craniotomy, (5) history of preexisting neurological disease, (6) previous hospitalization for TBI > 1 day, (7) bilaterally absent pupillary responses, (8) any contraindication to MRI, or (9) pregnant or member of a vulnerable population.

Initial MRI (scan A) was obtained at a median of 1 day (range 0.5 – 9) post-injury. Follow-up MRI (scan B) was performed at a median of 7.9 months (range 6 – 14). Five patients had substantial motion artifact on either scan A or B, and one patient did not return for follow-up. This resulted in 25 patients with complete data (Table 1). Twenty-two controls without a history of TBI or neurological disorder and selected to match the TBI group with respect to age and gender were scanned once. Demographic information for patients and controls is displayed in Table 2.

Imaging acquisition and analysis

Three-dimensional T1-weighted structural MPRAGE images were acquired on a GE Signa Excite 3T MRI scanner (General Electric Healthcare, Milwaukee, Wisconsin) using fast spoiled gradient-recalled acquisition in the steady state (GRASS) sequences (256 × 192 matrix size, 240 mm × 211 mm field of view, 130 slices, 1.3 mm slice thickness, no gap, 2.4 millisecond echo time, 25° flip angle, 2 excitations, 6 minute acquisition time). Image files were transferred to a Macintosh workstation for analysis with *FreeSurfer* (v4.5.0) image analysis suite (Athinoula A. Martinos Center for Biomedical Imaging, Charlestown, MA), which has been described in detail in prior publications.[21-24]

In brief, *FreeSurfer* analysis includes averaging of multiple volumetric T1-weighted images, removal of non-brain tissue, conversion to Talairach coordinates, automated segmentation of subcortical white and deep gray matter structures, tessellation of the gray-white matter junction, surface deformation along intensity gradients for optimal placement of gray-white and gray-cerebrospinal fluid (CSF) borders, and cortical parcellation with submillimeter precision into units based on gyral and sulcal structure. These procedures result in high-resolution quantification of thickness, surface area, and volume over the entire brain, in addition to delineating atlas-derived subcortical and cortical brain regions.

Functional Outcome

Functional outcome was assessed at time of follow-up MRI using the Glasgow Outcome Scale - Extended (GOSE). The GOSE provides an objective measure of recovery after TBI and is an ordinal scale from 1 to 8 with higher scores reflecting better outcomes. All follow-up interviews were conducted by one of three study coordinators with specific training and experience in interviewing patients with TBI, and interviews were conducted face-to-face. Inter-rater reliability was assessed by auditing 20% of scoring sheets every three months, with greater than 99% reproducibility.

Statistical Analyses

Volumetric differences between scans A and B were tested using repeated measures ANCOVA with correction for intracranial volume (ICV). Changes in volume between controls and patients were tested using ANCOVA with an ICV covariate. Cortical structures were reconstructed and voxel-wise volume changes between scans A and B were computed with *FreeSurfer's* general linear model for paired analysis using a 10-mm full-width half-maximum Gaussian kernel. A false discovery rate (FDR) of 0.05 was used for all analyses to account for effects of multiple comparisons. In order to determine candidate regions with prognostic value, correlations between atrophy rates and GOSE were calculated using Spearman's correlation coefficients and a screening FDR threshold of 0.10. Structures surviving the correlation analysis screen were entered into ordinal regression models for calculation of odds ratios of post-traumatic disability using volume change between scans A and B as the predictor variable and GOSE, trichotomized into severe disability (GOSE 3-4), moderate disability (GOSE 5-6), and good recovery (GOSE 7-8), as the dependent variable. All statistical analyses were performed with SPSS (v.11.5).

FreeSurfer morphometric analyses were conducted by 3 independent raters, and interrater reliability was determined by having each rater analyze 20 brains for determination of intraclass correlation coefficients (ICC) using two-way ANOVA with mixed effects. Regions having an ICC less than 0.850 or a single-rater coefficient of variation greater than 20% in controls, with the exception of the ventricles, were excluded from analyses.

RESULTS

Interrater reliability

The mean ICC for interrater reliability was 0.964 (median 0.978, range 0.855 – 0.999). Four cortical regions, the left and right temporal and frontal poles, and four subcortical structures, the left and right globus pallidum and accumbens area, had a coefficient of variation greater than 20% in controls and were excluded from analysis.

Global atrophy

All global measures of brain volume indicated loss of volume between scans A and B, with significant decreases in 9 of 12 measures (Table 3). Of note, whole brain parenchymal volume (WBPV) decreased by a mean of 4.5% (95% CI: 2.7 – 6.3) and whole white matter volume by 5.8% (3.2 – 8.4). There was substantial enlargement of all 4 ventricles and an increase in total CSF volume.

Subcortical Atrophy

Thirteen of 22 subcortical structures underwent atrophy after injury (Table 4), with the highest rates occurring bilaterally in the amygdala, which underwent mean volume loss of nearly 15%. Substantial atrophy was also seen in the thalamus, hippocampus, and putamen,

but not in the caudate or cerebellum. The corpus callosum was particularly vulnerable to volume loss.

Cortical atrophy

Of the 62 cortical regions analyzed by structural boundaries, atrophy was found in 13 (Table 5). Volume differences analyzed per brain voxel revealed substantial atrophy extending bilaterally into numerous regions including the superior frontal and rostral middle frontal cortex, superior and inferior parietal cortex, paracentral lobule, parsorbitalis, pericalcarine cortex, precuneus, cuneus, lingual cortex, and postcentral and supramarginal gyri (Figure 1). Loss of brain volume was most prominent in the precuneus, paracentral lobules, and parietal cortex.

Control group comparisons

In global comparisons between controls and acute scans, the lateral ventricles were significantly larger in the control group (Table 3). In subcortical and cortical analyses, there were no significant differences between controls and acutely injured patients (Tables 4 and 5).

Atrophy and Functional Outcome

Three global brain volume metrics and 14 subcortical and cortical regions survived a correlation analysis screen of atrophy rates and outcome. Odds ratios for disability with 10% volume loss were calculated for each (Table 6). WBPV and whole gray matter volume loss demonstrated prognostic value, as did atrophy in several brain regions. The probability of having disability (GOSE < 7) or severe disability (GOSE < 5) at follow-up was assessed for changes in WBPV (Table 7). With no change in WBPV the risk for disability was 10%, but this risk increased to 37% with 5% atrophy and 76% with 10% atrophy.

COMMENT

We prospectively and longitudinally assessed regional and global changes in gray and white matter volumes in patients with TAI scanned acutely and again several months after injury using *FreeSurfer* morphometry, while also investigating the relationship between atrophy and functional outcome. The distribution of atrophy was essentially symmetric. Substantial atrophy was observed in the cerebral cortex, subcortical structures, and white matter. Loss of WBPV was predictive of poor outcome, as was atrophy in several brain regions. This represents the first application of *FreeSurfer* morphometry in a longitudinal investigation of adult TBI.

Our findings of significant decreases in global brain volume after traumatic insult are consistent with previous studies. In a recent longitudinal study of 24 patients with severe TBI, brain parenchymal volume decreased by a mean of 4.0% between initial MRI at 8 weeks and follow-up MRI at 12 months.[10] Another longitudinal study of TBI patients with injuries ranging from mild to severe found a mean decrease in brain parenchymal volume of 1.43% between 11 weeks and 13 months post-injury.[16] Lastly, a smaller study of patients with mild and moderate TBI found a mean decrease in brain volume of 4.16% over any interval of at least 3 months, however the time to initial MRI varied from 7 to 430 days after trauma.[6] The loss of WBPV in our study (mean 4.5%) is higher than in prior studies. This is likely the consequence of obtaining the initial MRI earlier (median 1 day), therefore increasing our ability to detect atrophy in the acute and early subacute post-traumatic period. As noted previously, it is probable that the rate and distribution of atrophy are dependent on time after injury,[10] and higher atrophy rates may occur during the acute/early subacute period than during the late subacute/chronic period. In addition, differences in global

atrophy rates may be related to the automated methods used for morphometric analysis, which may result in minor variations in calculation of WBPV.[25]

Our study examined patients whose predominant injury mechanism was TAI, excluding those with focal lesions > 10 ml and those requiring cranial surgery. Even in the absence of focal trauma, there was substantial loss of brain volume, supporting the hypothesis that a primary mechanism of post-traumatic atrophy is diffuse white matter damage with secondary Wallerian degeneration and eventual neuronal cell death. A previous study from our group examined the relationship between acute measures of white matter integrity and global atrophy in patients with TAI, finding that acute axonal lesions (within 1 month of injury) measured by fluid attenuation inversion recovery (FLAIR) imaging were strongly predictive of atrophy at 6 months.[9] A recent study of patients with severe TBI, not limited to those with TAI, found the most substantial decreases in brain volume in regions susceptible to the consequences of TAI.[10] However, since conventional neuroimaging techniques including CT and structural MRI have low sensitivity for TAI, it is likely that patients with focal hematomas also had significant diffuse axonal injuries, potentially explaining the similarities between our findings and previous work.[6,10,16] In order to improve post-traumatic outcomes, it will be essential to advance clinical detection and diagnosis of TAI.

Post-traumatic atrophy was not uniformly diffuse. Amongst subcortical structures, the highest rates of atrophy were noted bilaterally in the amygdala, hippocampus, thalamus, and putamen. Atrophy in the thalamus and putamen have been observed in several previous TBI studies.[13,14,26] Loss of volume in the amygdala and hippocampus may contribute to various behavioral and cognitive difficulties that commonly affect head-injured patients such as lability of mood, heightened irritability, and difficulties with memory and learning.

In cortical analysis, a variety of regions experienced marked atrophy, with the most dramatic volume loss occurring in the parietal lobes, superior frontal lobes, precuneus, and paracentral lobules. A recent longitudinal study found decreased volume in the supplementary motor area and pre- and post-central gyri,[14] while another found atrophy only in small portions of the frontal cortex.[10] The apparent disparity in degree of cortical atrophy in our study versus previous studies is likely due to inter-subject variability in cortical sulci and gyri that make volumetric analysis of the cortex exceptionally difficult with traditional voxel-wise approaches. The application of *FreeSurfer* morphometry to this study improves the ability to delineate and quantify the cerebral cortex at the subvoxel level, resulting in increased sensitivity for cortical volume loss. In addition, previous studies have not excluded patients with focal lesions that may further obscure cortical morphometry. Although extensive, cortical atrophy was not diffuse, and several regions, including the entorhinal cortex, parahippocampal gyrus, and fusiform gyrus, were resilient to atrophy. Larger studies with increased follow-up times will be needed to improve the detection and quantification of regional volume changes after TAI.

Regionally selective cortical and subcortical atrophy has been studied extensively in Alzheimer's disease, and we note that many of the areas that are particularly susceptible to atrophy in Alzheimer's disease are also vulnerable after TAI. For example, in addition to hippocampal volume loss, patients with Alzheimer's disease have high rates of atrophy in the amygdala,[27-29] precuneus, parietal, and frontal cortex,[30-32] and corpus callosum.[33-36] While interesting, the relationship is far from perfect, and some regions that undergo substantial atrophy in Alzheimer's disease, such as the medial-inferior temporal lobe, may be relatively preserved after TAI. However, it is plausible that regional similarities in atrophy between TAI and Alzheimer's disease may contribute to post-traumatic deficits in certain cognitive domains such as learning and memory. We also note that many brain regions vulnerable to atrophy in our study and in Alzheimer's disease are involved in the

default network.[32] These findings may relate to common molecular mechanisms shared between Alzheimer's disease and TBI-related neurodegeneration.

As expected, loss of WBPV was predictive of disability at time of patient follow-up, with a nearly 30-fold increase in disability risk in patients with 10% atrophy. In addition, volume loss in several candidate brain regions displayed prognostic value for outcome, suggesting that regional morphometry may hold value as a biomarker for recovery after trauma. While interesting, our analysis involved only a small number of patients and was by no means exhaustive. In order to better understand the influence of regional volume changes on patient outcomes, it will be necessary to assess atrophy-outcome relationships for a greater number of brain regions in a larger number of patients with more precise metrics of functional recovery after brain trauma such as neuropsychological battery tests.

There are several limitations to our study. We assessed longitudinal changes in brain volumes between the acute and late subacute time periods. As the brain may swell acutely after injury, it is possible that the clearing of brain edema may contribute to observed losses of brain volume. However, in cross-sectional comparisons between control and acute patient scans, there were no significant differences in cortical or subcortical brain volumes. The only significant difference between groups was volume of the lateral ventricles, which were larger in controls, suggesting that there may be diffuse swelling after injury. However, as ventricular enlargement is at best an indirect measurement of atrophy, it is much less sensitive than direct measurement of changes in structural volumes.[13] Therefore, it is unlikely that brain edema played a substantial role in observed decreases in brain volume. This study contained only a modest sample size, and in order to further our understanding of atrophy after TAI, it will be necessary to enroll a larger number of patients. In addition, follow-up MRI scans were not performed on controls, which would have permitted more robust comparisons between independent groups. Controls and patients were matched based on gender and age, but not on years of education. This resulted in a control group with a significantly higher education level, which could potentially confound between-group comparisons. Finally, this longitudinal study utilized two time points for quantitative MRI, and only assessed atrophy that occurred between the acute and late subacute time periods. In order to more fully understand the time course and regional distribution of post-traumatic atrophy, it will be necessary to obtain additional serial MRI scans at shorter time intervals and over a longer study time period.

This prospective evaluation of longitudinal changes in brain volumes after TAI offers new information on the spatial distribution of post-traumatic cerebral atrophy. Our findings indicate that atrophy is not uniformly diffuse, but rather has substantial selectivity for various subcortical and cortical regions including the amygdala, hippocampus, thalamus, precuneus, parietal, and frontal cortex. Atrophy in several brain regions may be also be predictive of long-term functional recovery. Future studies will be needed to determine the impact of regional atrophy on particular neuropsychological outcomes. Finally, it will be necessary to integrate regional volumetric data with measurements of axonal integrity in order to assess the true relationship between acute white matter injury and chronic volume loss in corresponding gray matter.

Acknowledgments

We would like to acknowledge the contributions of Dr. Evelyn Babcock, PhD for her technical support with image acquisition and quality control.

Funding/Support: This study was supported by a Clinical Research Fellowship through the Doris Duke Charitable Foundation (Mr. Warner and Dr. Youn), grants R01 HD48179 and U01 HD42652 from the National Institutes of

Health – National Institute of Child Health and Human Development (Dr. Diaz-Arrastia), and grant H133 A020526 from the United States Department of Education (Dr. Diaz-Arrastia).

REFERENCES

1. Langlois, J.; Rutland-Brown, W.; Thomas, K. Traumatic Brain Injury in the United States: Emergency Department Visits, Hospitalizations, and Deaths. National Center for Injury Prevention and Control; Atlanta, GA: 2006.
2. Ariza M, Serra-Grabulosa JM, Junque C, et al. Hippocampal head atrophy after traumatic brain injury. Neuropsychologia. 2006; 44(10):1956–1961. [PubMed: 16352320]
3. Bigler ED. Quantitative magnetic resonance imaging in traumatic brain injury. J Head Trauma Rehabil. Apr; 2001 16(2):117–134. [PubMed: 11275574]
4. Bigler ED, Ryser DK, Gandhi P, Kimball J, Wilde EA. Day-of-injury computerized tomography, rehabilitation status, and development of cerebral atrophy in persons with traumatic brain injury. Am J Phys Med Rehabil. Oct; 2006 85(10):793–806. [PubMed: 16998426]
5. Gale SD, Baxter L, Roundy N, Johnson SC. Traumatic brain injury and grey matter concentration: a preliminary voxel based morphometry study. J Neurol Neurosurg Psychiatry. Jul; 2005 76(7):984–988. [PubMed: 15965207]
6. MacKenzie JD, Siddiqi F, Babb JS, et al. Brain atrophy in mild or moderate traumatic brain injury: a longitudinal quantitative analysis. AJNR Am J Neuroradiol. Oct; 2002 23(9):1509–1515. [PubMed: 12372740]
7. Tomaiuolo F, Carlesimo GA, Di Paola M, et al. Gross morphology and morphometric sequelae in the hippocampus, fornix, and corpus callosum of patients with severe non-missile traumatic brain injury without macroscopically detectable lesions: a T1 weighted MRI study. J Neurol Neurosurg Psychiatry. Sep; 2004 75(9):1314–1322. [PubMed: 15314123]
8. Tomaiuolo F, Worsley KJ, Lerch J, et al. Changes in white matter in long-term survivors of severe non-missile traumatic brain injury: a computational analysis of magnetic resonance images. J Neurotrauma. Jan; 2005 22(1):76–82. [PubMed: 15665603]
9. Ding K, Marquez de la Plata C, Wang JY, et al. Cerebral atrophy after traumatic white matter injury: correlation with acute neuroimaging and outcome. J Neurotrauma. Dec; 2008 25(12):1433–1440. [PubMed: 19072588]
10. Sidaros A, Skimminge A, Liptrot MG, et al. Long-term global and regional brain volume changes following severe traumatic brain injury: a longitudinal study with clinical correlates. Neuroimage. Jan 1; 2009 44(1):1–8. [PubMed: 18804539]
11. Povlishock JT, Katz DI. Update of neuropathology and neurological recovery after traumatic brain injury. J Head Trauma Rehabil. Jan-Feb;2005 20(1):76–94. [PubMed: 15668572]
12. Merkley TL, Bigler ED, Wilde EA, McCauley SR, Hunter JV, Levin HS. Diffuse changes in cortical thickness in pediatric moderate-to-severe traumatic brain injury. J Neurotrauma. Nov; 2008 25(11):1343–1345. [PubMed: 19061377]
13. Kim J, Avants B, Patel S, et al. Structural consequences of diffuse traumatic brain injury: a large deformation tensor-based morphometry study. Neuroimage. Feb 1; 2008 39(3):1014–1026. [PubMed: 17999940]
14. Bendlin BB, Ries ML, Lazar M, et al. Longitudinal changes in patients with traumatic brain injury assessed with diffusion-tensor and volumetric imaging. Neuroimage. Aug 15; 2008 42(2):503–514. [PubMed: 18556217]
15. Salmond CH, Chatfield DA, Menon DK, Pickard JD, Sahakian BJ. Cognitive sequelae of head injury: involvement of basal forebrain and associated structures. Brain. Jan; 2005 128(Pt 1):189–200. [PubMed: 15548553]
16. Trivedi MA, Ward MA, Hess TM, et al. Longitudinal changes in global brain volume between 79 and 409 days after traumatic brain injury: relationship with duration of coma. J Neurotrauma. May; 2007 24(5):766–771. [PubMed: 17518532]
17. McDonald CR, Hagler DJ Jr. Ahmadi ME, et al. Subcortical and cerebellar atrophy in mesial temporal lobe epilepsy revealed by automatic segmentation. Epilepsy Res. May; 2008 79(2-3): 130–138. [PubMed: 18359198]

18. Pengas G, Pereira JM, Williams GB, Nestor PJ. Comparative reliability of total intracranial volume estimation methods and the influence of atrophy in a longitudinal semantic dementia cohort. J Neuroimaging. Jan; 2009 19(1):37–46. [PubMed: 18494772]
19. Holland D, Brewer JB, Hagler DJ, et al. Subregional neuroanatomical change as a biomarker for Alzheimer's disease. Proc Natl Acad Sci U S A. Dec 8; 2009 106(49):20954–20959. [PubMed: 19996185]
20. Tae WS, Kim SS, Lee KU, Nam EC, Kim KW. Validation of hippocampal volumes measured using a manual method and two automated methods (FreeSurfer and IBASPM) in chronic major depressive disorder. Neuroradiology. Jul; 2008 50(7):569–581. [PubMed: 18414838]
21. Dale AM, Fischl B, Sereno MI. Cortical surface-based analysis. I. Segmentation and surface reconstruction. Neuroimage. Feb; 1999 9(2):179–194. [PubMed: 9931268]
22. Fischl B, Dale AM. Measuring the thickness of the human cerebral cortex from magnetic resonance images. Proc Natl Acad Sci U S A. Sep 26; 2000 97(20):11050–11055. [PubMed: 10984517]
23. Fischl B, Sereno MI, Dale AM. Cortical surface-based analysis. II: Inflation, flattening, and a surface-based coordinate system. Neuroimage. Feb; 1999 9(2):195–207. [PubMed: 9931269]
24. Fischl B, Salat DH, Busa E, et al. Whole brain segmentation: automated labeling of neuroanatomical structures in the human brain. Neuron. Jan 31; 2002 33(3):341–355. [PubMed: 11832223]
25. van der Kouwe AJ, Benner T, Salat DH, Fischl B. Brain morphometry with multiecho MPRAGE. Neuroimage. Apr 1; 2008 40(2):559–569. [PubMed: 18242102]
26. Sidaros A, Engberg AW, Sidaros K, et al. Diffusion tensor imaging during recovery from severe traumatic brain injury and relation to clinical outcome: a longitudinal study. Brain. Feb; 2008 131(Pt 2):559–572. [PubMed: 18083753]
27. Teipel SJ, Pruessner JC, Faltraco F, et al. Comprehensive dissection of the medial temporal lobe in AD: measurement of hippocampus, amygdala, entorhinal, perirhinal and parahippocampal cortices using MRI. J Neurol. Jun; 2006 253(6):794–800. [PubMed: 16511646]
28. Shiino A, Watanabe T, Kitagawa T, et al. Different atrophic patterns in early- and late-onsetalzheimer's disease and evaluation of clinical utility of a method of regional z-score analysis using voxel-based morphometry. Dement Geriatr Cogn Disord. 2008; 26(2):175–186. [PubMed: 18698140]
29. Basso M, Yang J, Warren L, et al. Volumetry of amygdala and hippocampus and memory performance in Alzheimer's disease. Psychiatry Res. Apr 30; 2006 146(3):251–261. [PubMed: 16524704]
30. Agosta F, Vossel KA, Miller BL, et al. Apolipoprotein E epsilon4 is associated with disease-specific effects on brain atrophy in Alzheimer's disease and frontotemporal dementia. Proc Natl Acad Sci U S A. Feb 10; 2009 106(6):2018–2022. [PubMed: 19164761]
31. Scahill RI, Schott JM, Stevens JM, Rossor MN, Fox NC. Mapping the evolution of regional atrophy in Alzheimer's disease: unbiased analysis of fluid-registered serial MRI. Proc Natl Acad Sci U S A. Apr 2; 2002 99(7):4703–4707. [PubMed: 11930016]
32. Buckner RL, Snyder AZ, Shannon BJ, et al. Molecular, structural, and functional characterization of Alzheimer's disease: evidence for a relationship between default activity, amyloid, and memory. J Neurosci. Aug 24; 2005 25(34):7709–7717. [PubMed: 16120771]
33. Teipel SJ, Bayer W, Alexander GE, et al. Progression of corpus callosum atrophy in Alzheimer disease. Arch Neurol. Feb; 2002 59(2):243–248. [PubMed: 11843695]
34. Teipel SJ, Bayer W, Alexander GE, et al. Regional pattern of hippocampus and corpus callosum atrophy in Alzheimer's disease in relation to dementia severity: evidence for early neocortical degeneration. Neurobiol Aging. Jan-Feb;2003 24(1):85–94. [PubMed: 12493554]
35. Wang PJ, Saykin AJ, Flashman LA, et al. Regionally specific atrophy of the corpus callosum in AD, MCI and cognitive complaints. Neurobiol Aging. Nov; 2006 27(11):1613–1617. [PubMed: 16271806]
36. Yamauchi H, Fukuyama H, Nagahama Y, et al. Comparison of the pattern of atrophy of the corpus callosum in frontotemporal dementia, progressive supranuclear palsy, and Alzheimer's disease. J Neurol Neurosurg Psychiatry. Nov; 2000 69(5):623–629. [PubMed: 11032614]

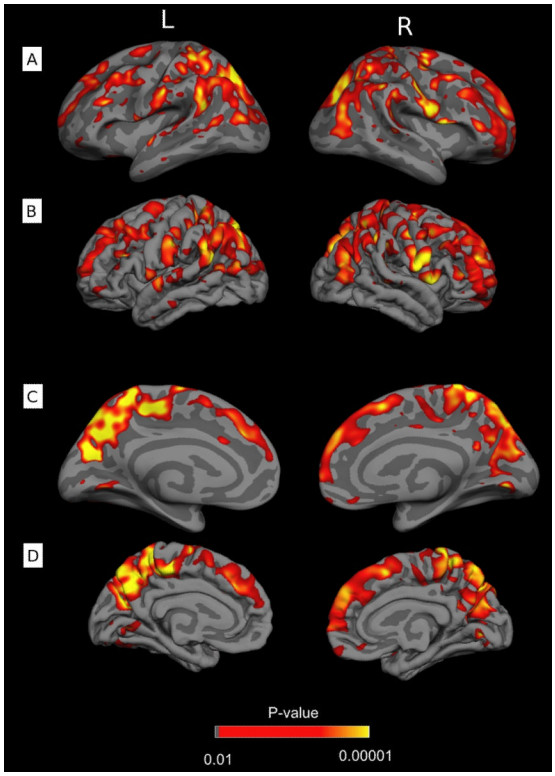

Figure 1.
Regions of significant cortical atrophy between initial (median 1 day) and follow-up MRI (median 7.9 months) in 25 adults with diffuse traumatic axonal injury. Highlighted regions are significant at a false discovery rate of 0.05. A) Lateral view, inflated to show extent of cortical surface; B) Lateral view, displayed at the pial layer; C) Midsagittal view, inflated; D) Midsagittal view, pial layer.

Table 1

Clinical characteristics of patients

Patient	Age	Sex	Cause of Trauma	GCS	Head AIS	ISS	ICU Days	Hospital Days	Scan A (days)	Scan B (months)	GOSE	FSE
1	17	M	MVC	3	3	10	13	15	4	11	8	15
2	32	M	MCC	3	3	14	12	40	8	9	3	36
3	17	F	MVC	3	3	25	4	7	5	9	8	10
4	17	M	MVC	3	4	21	10	31	9	9	5	18
5	36	F	MVC	3	5	38	13	18	9	9	3	31
6	20	F	MVC	8	4	17	18	18	2	7	3	32
7	20	M	MVC	6	3	10	24	25	5	8	7	12
8	27	M	MVC	3	4	29	19	34	0.5	14	6	21
9	16	F	MVC	10	3	38	2	11	1	6	8	10
10	40	F	MVC	8	5	50	5	11	1	9	8	10
11	28	M	MVC	15	4	29	3	7	1	6	6	18
12	32	M	MCC	6	5	38	4	23	1	6	4	26
13	23	M	MCC	8	5	50	1	2	1	6	7	10
14	17	F	MVC	15	3	14	1	2	0.5	6	8	10
15	20	M	MVC	3	5	38	2	7	1	7	3	27
16	40	M	MCC	3	4	34	7	14	2.5	8	7	18
17	23	F	MVC	8	4	36	15	22	1.5	6	5	25
18	18	M	MVC	3	4	41	3	8	2	8	8	16
19	27	M	MVC	8	4	17	3	12	1	8	8	10
20	23	M	MVC	3	4	20	3	12	0.5	7	7	13
21	18	M	WSI	3	4	17	2	4	1	8	8	13
22	58	M	MVC	15	5	34	1	2	1	6	6	14
23	54	M	MPC	3	4	24	3	6	1	6	7	19
24	23	M	MCC	10	5	43	2	6	2	7	8	19
25	23	M	MPC	3	3	17	1	5	1	8	8	11
			Mean	6.2	4.0	28.2	6.8	13.6	2.5	7.8	6.4	17.8
			SD	4.5	0.8	12.2	6.7	10.4	2.6	1.9	1.9	7.7
			Median	4.1	4.0	29.0	3.0	11.0	1.0	7.9	7.0	16.0

MVC = motor vehicle collision; MCC = motorcycle collision; MPC = motor vehicle – pedestrian collision; WSI = water sports incident; GCS = Post-resuscitation Glasgow coma scale; AIS = abbreviated injury scale; ISS = injury severity score; ICU = intensive care unit; Scan A = initial MRI; Scan B = follow-up MRI; GOSE = Glasgow outcome scale – extended; FSE = functional status examination; SD = standard deviation; See text for details.

Table 2

Demographic characteristics of patients and controls

	Patients (n = 25)	Controls (n = 22)	Group differences
Age, Scan A (years), mean (SD)	26.8 (11.3)	32.4 (13.5)	P = 0.125 *
Sex: M/F	18/7	14/8	P = 0.775 #
Education (years), mean (SD)	12.2 (2.4)	15.8 (3.1)	**P < 0.001** *

* Independent-samples T-test;

Fisher's Exact Test;

Scan A = initial MRI. P-values in bold are significant at P < 0.05

Table 3

Global measures of brain volume in TBI patients at initial scan and follow-up scan, and in normal controls

	TBI-A	TBI-B	% Change	A-B P-value*	Control	Control-A P-value#
ICV	1563.6 ± 155.9	1552.2 ± 170.3	−0.9	0.568	1514.3 ± 156.2	0.285
WBPV	1346.8 ± 134.3	1287.6 ± 146.2	−4.5	**0.002**	1318.5 ± 107.3	0.338
WGMV	755.2 ± 77.5	722.2 ± 91.2	−3.7	0.056	742.8 ± 67.3	0.123
WWMV	564.0 ± 73.4	531.4 ± 66.9	−5.8	**0.003**	547.8 ± 61.3	0.579
Lateral Ventricle - L	4.5 ± 3.4	8.2 ± 4.8	+82.3	**<0.001**	7.8 ± 4.4	**<0.001**
Lateral Ventricle - R	4.8 ± 3.4	7.4 ± 3.5	+80.2	**<0.001**	7.0 ± 4.8	**<0.001**
3rd Ventricle	0.9 ± 0.3	1.3 ± 0.5	+54.0	**<0.001**	1.1 ± 0.4	0.074
4th Ventricle	1.8 ± 0.6	2.3 ± 0.6	+27.5	**0.005**	2.1 ± 0.7	0.139
CSF	1.4 ± 0.3	1.8 ± 0.3	+36.9	**<0.001**	1.6 ± 0.4	0.008
Cerebral Cortex - L	288.8 ± 32.2	280.0 ± 39.6	−3.0	0.162	279.7 ± 27.7	0.071
Cerebral Cortex - R	284.1 ± 32.7	274.7 ± 36.2	−3.3	0.157	278.6 ± 28.5	0.052
Cerebral WM - L	266.0 ± 35.0	250.0 ± 32.1	−6.0	**0.004**	256.9 ± 30.8	0.127
Cerebral WM - R	268.0 ± 36.9	252.1 ± 33.8	−5.9	**0.006**	260.1 ± 29.4	0.460

*Repeated measures ANCOVA correcting for ICV;

#ANCOVA correcting for ICV;

P-values in bold are significant at a false discovery rate of 0.05. All volumes were normalized to control ICV to allow for cross-comparisons. Volumes are in cubic millimeters. TBI-A = patient initial MRI; TBI-B = patient follow-up MRI; ICV = intracranial volume; WBPV = whole brain parenchymal volume; WGMV = whole gray matter volume; WWMV = whole white matter volume; CSF = cerebrospinal fluid; WM = white matter; L = left; R = right.

Table 4

Subcortical brain volumes in TBI patients at initial scan and follow-up scan, and in normal controls

	TBI-A	TBI-B	% Change	A-B P-value*	Control	Control-A P-value#
Amygdala - L	1.8 ± 0.3	1.5 ± 0.2	−14.6	**<0.001**	1.7 ± 0.2	0.508
Amygdala - R	1.7 ± 0.3	1.4 ± 0.3	−15.0	**<0.001**	1.7 ± 0.3	0.646
Brain Stem	21.2 ± 2.1	19.9 ± 2.1	−6.0	**0.014**	21.9 ± 2.5	0.102
Caudate - L	3.8 ± 0.5	3.7 ± 0.5	−2.9	0.281	3.8 ± 0.6	0.204
Caudate - R	3.7 ± 0.6	3.4 ± 0.6	−7.4	0.065	3.7 ± 0.5	0.820
Cerebellum Cortex - L	59.9 ± 6.4	59.7 ± 7.1	−0.3	0.401	62.1 ± 5.4	0.282
Cerebellum Cortex - R	61.4 ± 6.6	59.7 ± 7.3	−2.8	0.181	64.0 ± 6.1	0.287
Cerebellum WM - L	15.6 ± 2.1	14.9 ± 2.0	−3.4	0.284	15.8 ± 2.2	0.518
Cerebellum WM - R	14.9 ± 2.1	14.2 ± 1.7	−4.8	0.139	15.4 ± 2.1	0.218
CC anterior	0.83 ± 0.22	0.79 ± 0.18	−4.1	0.091	0.88 ± 0.17	0.846
CC middle anterior	0.52 ± 0.11	0.41 ± 0.09	−21.4	**<0.001**	0.48 ± 0.09	0.042
CC central	0.50 ± 0.11	0.43 ± 0.12	−13.6	**0.010**	0.46 ± 0.09	0.012
CC middle posterior	0.50 ± 0.11	0.42 ± 0.08	−16.8	**0.002**	0.46 ± 0.11	0.007
CC posterior	0.86 ± 0.19	0.84 ± 0.20	−3.2	0.023	0.97 ± 0.12	0.435
Hippocampus - L	4.8 ± 0.5	4.3 ± 0.7	−9.8	**0.001**	4.6 ± 0.6	0.856
Hippocampus - R	4.8 ± 0.6	4.2 ± 0.7	−11.2	**<0.001**	4.6 ± 0.5	0.303
Putamen - L	5.6 ± 0.9	5.0 ± 0.9	−10.4	0.019	5.2 ± 1.0	0.440
Putamen - R	5.4 ± 0.8	4.6 ± 0.5	−14.3	**<0.001**	5.0 ± 1.0	0.242
Thalamus - L	8.4 ± 1.0	7.3 ± 1.0	−12.6	**<0.001**	8.1 ± 0.9	0.683
Thalamus - R	8.3 ± 1.0	7.4 ± 1.1	−10.4	**<0.001**	8.2 ± 1.0	0.571
Ventral Diencephalon - L	4.3 ± 0.4	4.1 ± 0.6	−6.6	**0.008**	4.3 ± 0.5	0.988
Ventral Diencephalon - R	4.3 ± 0.5	3.9 ± 0.5	−9.3	**0.002**	4.2 ± 0.5	0.900

*Repeated measures ANCOVA correcting for ICV;

#ANCOVA correcting for ICV;

P-values in bold are significant at a false discovery rate of 0.05. All volumes were normalized to control ICV to allow for cross-comparisons. Volumes are in cubic millimeters. TBI-A = patient initial MRI; TBI-B = patient follow-up MRI; L = left; R = right; WM = white matter; CC = corpus callosum.

Table 5

Cortical brain volumes in TBI patients at initial scan and follow-up scan, and in normal controls

	TBI-A	TBI-B	% Change	A-B P-value*	Control	Control-A P-value#
Anterior Cingulate - Caudal L	1.9 ± 0.5	1.7 ± 0.4	−12.7	0.030	1.9 ± 0.4	0.216
Anterior Cingulate - Caudal R	2.0 ± 0.6	2.2 ± 0.6	+6.0	0.278	2.0 ± 0.5	0.156
Anterior Cingulate - Rostral L	2.3 ± 0.6	2.2 ± 0.5	−3.8	0.332	2.2 ± 0.5	0.975
Anterior Cingulate - Rostral R	1.8 ± 0.4	1.9 ± 0.4	+7.0	0.690	2.1 ± 0.4	0.225
Cuneus - L	3.0 ± 0.8	2.8 ± 0.6	−8.9	0.072	3.0 ± 0.5	0.411
Cuneus - R	3.5 ± 0.7	2.9 ± 0.6	−14.9	**0.009**	3.2 ± 0.8	0.006
Entorhinal - L	1.4 ± 0.4	1.4 ± 0.4	−0.5	0.772	1.5 ± 0.4	0.332
Entorhinal - R	1.3 ± 0.3	1.3 ± 0.4	+2.0	0.904	1.3 ± 0.5	0.820
Middle Frontal - Caudal L	6.9 ± 1.8	6.7 ± 1.6	−3.8	0.459	6.8 ±.1.3	0.409
Middle Frontal - Caudal R	6.8 ± 1.4	6.1 ± 1.4	−10.0	0.040	6.8 ± 1.3	0.574
Middle Frontal - Rostral L	17.6 ± 4.0	16.2 ± 3.8	−8.1	0.076	17.0 ± 2.8	0.316
Middle Frontal - Rostral R	17.0 ± 3.3	16.0 ± 3.3	−6.3	0.187	17.5 ± 3.0	0.401
Superior Frontal - L	23.9 ± 4.5	21.6 ± 3.6	−9.2	0.024	23.9 ± 3.3	0.504
Superior Frontal - R	23.9 ± 4.0	20.9 ± 4.4	−12.4	**0.002**	22.6 ± 3.8	0.128
Fusiform - L	9.7 ± 2.0	9.4 ± 2.1	−3.5	0.509	10.0 ± 1.4	0.621
Fusiform - R	8.8 ± 1.4	8.7 ± 1.6	−0.5	0.609	9.2 ± 1.4	0.467
Insula - L	6.6 ± 1.0	6.6 ± 0.9	0.0	0.934	6.9 ± 0.8	0.346
Insula - R	6.4 ± 0.6	6.3 ± 0.8	−1.4	0.247	6.9 ± 0.5	0.100
Isthmuscingulate - L	2.5 ± 0.5	2.5 ± 0.5	−1.5	0.750	2.5 ± 0.4	0.516
Isthmuscingulate - R	2.4 ± 0.5	2.3 ± 0.5	−2.7	0.461	2.2 ± 0.4	0.424
Lingual - L	6.7 ± 1.3	6.5 ± 1.3	−1.4	0.724	6.8 ± 0.8	0.327
Lingual - R	6.7 ± 1.1	6.6 ± 1.2	−1.6	0.115	6.8 ± 0.4	0.444
Lateral Occipital - L	14.4 ± 2.8	13.0 ± 3.0	−9.7	0.032	13.9 ± 2.2	0.951
Lateral Occipital - R	13.7 ± 3.2	12.9 ± 2.4	−5.9	0.188	13.8 ± 2.1	0.912
Lateral Orbitofrontal - L	7.3 ± 0.9	6.9 ± 1.2	−6.4	0.039	7.0 ± 1.1	0.097
Lateral Orbitofrontal - R	7.3 ± 1.0	7.1 ± 1.4	−3.2	0.086	7.3 ± 0.7	0.512
Medial Orbitofrontal - L	4.6 ± 0.8	4.5 ± 0.8	−2.5	0.538	4.8 ± 0.8	0.751
Medial Orbitofrontal - R	4.7 ± 0.7	4.7 ± 0.7	0.0	0.535	5.0 ± 0.8	0.523

	TBI-A	TBI-B	% Change	A-B P-value*	Control	Control-A P-value#
Paracentral Lobule - L	3.5 ± 0.6	3.2 ± 0.6	−9.2	**0.003**	3.4 ± 0.6	0.007
Paracentral Lobule - R	4.0 ± 0.8	3.5 ± 0.7	−11.4	**0.014**	3.8 ± 0.4	0.250
Parahippocampal - L	2.1 ± 0.6	2.1 ± 0.5	+1.6	0.321	2.2 ± 0.3	0.086
Parahippocampal - R	2.0 ± 0.4	2.0 ± 0.4	+1.8	0.794	1.9 ± 0.4	0.460
Pars opercularis - L	5.2 ± 1.1	5.2 ± 1.1	+0.5	0.947	5.3 ± 0.8	0.198
Pars opercularis - R	4.6 ± 1.0	4.2 ± 1.2	−8.9	0.042	4.2 ± 0.7	0.206
Pars orbitalis – L	2.3 ± 0.6	2.1 ± 0.6	−7.9	0.194	2.2 ± 0.6	0.335
Pars orbitalis – R	2.9 ± 0.8	2.5 ± 0.7	−12.2	0.037	2.6 ± 0.6	0.442
Pars triangularis - L	3.9 ± 1.0	3.7 ± 0.9	−6.8	0.240	4.5 ± 1.0	0.073
Pars triangularis - R	4.8 ± 1.2	4.2 ± 1.0	−11.4	0.028	5.1 ± 1.1	0.075
Inferior Parietal - L	14.3 ± 2.4	13.1 ± 2.3	−8.6	0.036	14.4 ± 2.5	0.129
Inferior Parietal - R	16.7 ± 2.1	15.1 ± 2.2	−9.4	**0.004**	16.5 ± 2.7	0.429
Superior Parietal - L	14.6 ± 2.6	12.4 ± 2.5	−15.1	<**0.001**	13.8 ± 1.5	0.007
Superior Parietal - R	14.1 ± 2.4	12.0 ± 2.3	−14.8	<**0.001**	13.6 ± 1.7	0.085
Pericalcarine – L	2.0 ± 0.6	1.8 ± 0.4	−10.9	0.023	1.8 ± 0.3	0.074
Pericalcarine - R	2.3 ± 0.4	2.1 ± 0.4	−7.5	0.057	2.1 ± 0.4	0.013
Posterior Cingulate - L	3.7 ± 0.5	3.4 ± 0.6	−7.2	0.038	3.6 ± 0.5	0.120
Posterior Cingulate - R	3.5 ± 0.7	3.4 ± 0.6	−1.7	0.494	3.6 ± 0.5	0.614
Postcentral – L	10.0 ± 2.0	8.9 ± 1.8	−10.7	**0.017**	9.5 ± 1.6	0.407
Postcentral – R	9.3 ± 1.4	8.3 ± 1.3	−9.4	**0.009**	9.0 ± 1.2	0.289
Precentral – L	12.7 ± 1.6	12.0 ± 2.0	−5.3	0.152	13.1 ± 1.6	0.788
Precentral – R	12.9 ± 1.8	12.2 ± 1.9	−4.7	0.377	13.1 ± 1.5	0.837
Precuneus – L	10.4 ± 1.6	8.7 ± 2.3	−16.1	**0.001**	9.6 ± 1.4	0.083
Precuneus – R	9.9 ± 1.7	9.1 ± 1.4	−8.0	**0.015**	10.1 ± 1.3	0.940
Supramarginal - L	10.9 ± 1.6	10.4 ± 1.9	−4.3	0.292	10.8 ± 1.8	0.831
Supramarginal - R	11.2 ± 1.8	10.1 ± 1.6	−9.9	**0.010**	10.7 ± 1.9	0.284
Inferior Temporal - L	10.6 ± 1.8	10.8 ± 2.2	+1.6	0.876	11.2 ± 2.0	0.370
Inferior Temporal - R	10.7 ± 2.0	10.5 ± 2.5	−1.1	0.649	10.9 ± 2.4	0.943
Medial Temporal - L	11.9 ± 1.4	11.3 ± 1.8	−4.8	**0.017**	12.7 ± 1.5	0.125
Medial Temporal - R	12.8 ± 2.1	12.3 ± 1.9	−3.7	0.366	13.8 ± 2.4	0.315
Superior Temporal - L	12.9 ± 1.5	12.0 ± 2.0	−6.9	0.034	14.1 ± 1.9	0.026

	TBI-A	TBI-B	% Change	A-B P-value*	Control	Control-A P-value#
Superior Temporal - R	11.6 ± 1.2	11.2 ± 1.8	−3.5	0.058	13.0 ± 1.4	0.007
Transverse Temporal - L	1.2 ± 0.3	1.1 ± 0.4	−2.8	0.503	1.3 ± 0.2	0.480
Transverse Temporal - R	0.9 ± 0.2	0.9 ± 0.2	−7.6	0.137	1.0 ± 0.2	0.709

*Repeated measures ANCOVA correcting for ICV;

#ANCOVA correcting for ICV;

P-values in bold are significant at a false discovery rate of 0.05. All volumes were normalized to control ICV to allow for cross-comparisons. Volumes are in cubic millimeters. TBI-A = patient initial MRI; TBI-B = patient follow-up MRI; L = left; R = right; WM = white matter.

Table 6

Odds ratios for disability with 10% volume loss in selected brain regions

	Odds Ratio*	Lower boundary of 95% CI
WBPV	27.39	2.65
WGMV	6.66	1.37
Cerebral Cortex - L	3.37	1.01
Putamen - L	1.42	0.96
CC central	1.55	0.97
CC anterior	1.61	0.91
Cuneus - L	1.73	1.09
Superior Frontal - R	1.96	0.98
Inferior Parietal - L	3.45	1.38
Superior Parietal - R	1.39	0.80
Pars orbitalis - R	2.19	1.19
Pericalcarine - L	1.98	1.11
Precentral - L	2.47	1.16
Precuneus - L	1.72	0.89
Precuneus - R	1.88	0.99
Supramarginal - L	2.77	1.16
Supramarginal - R	2.35	1.21

*Odds ratios were computed with ordinal logistic regression using the Glasgow Outcome Scale – Extended (GOSE), trichotomized into severe disability (GOSE 3-4), moderate disability (GOSE 5-6), and good recovery (GOSE 7-8), as the dependent variable. Reported values signify that for every 10% loss in regional brain volume, the odds of having moderate or severe disability will increase by a factor of (x). WBPV = whole brain parenchymal volume; WGMV = whole gray matter volume; L = left; R = right; CC = corpus callosum.

Table 7

Probability of disability with loss of whole brain parenchymal volume after traumatic axonal injury*

	Any Disability#	Severe Disability^
No atrophy	0.10	0.03
5% atrophy	0.37	0.15
10% atrophy	0.76	0.48

*Probabilities of disability were computed with ordinal logistic regression using whole brain parenchymal volume as the continuous predictor variable and Glasgow Outcome Scale – Extended (GOSE), trichotomized into severe disability (GOSE 3-4), moderate disability (GOSE 5-6), and good recovery (GOSE 7-8), as the dependent variable.

#Any disability = probability that a patient will have moderate or severe disability (GOSE 3-6).

^Severe disability = probability that a patient will have severe disability (GOSE 3-4).